Aluminum Buffering of Mildly Acidic Waste Rock from a Hard Rock, Open Pit Mine in the Central Rocky Mountains

Justin S. Stockwell and John W. Dockrey

Lorax Environmental Services Limited, 2289 Burrard Street, Vancouver, BC, Canada Justin.Stockwell@Lorax.ca

Abstract
Long-term water quality from a 25 year old waste rock dump in the central Rocky Mountains is examined to illustrate the evolution of mildly acidic drainage (approx. pH 4.5). As the primary repository of potentially acid generating waste rock, this dump was investigated to determine the mineral phases controlling pH. Samples obtained for this investigation included boreholes sampled at regular intervals throughout the dump profile, pore water extractions, ground water sampling within the base of the dump interior, and drainage monitoring at the toe. Solid phase samples were analyzed with SEM-EDS, XRD, and standard ABA testing. The pH in the interior of the dump was found to be bimodal, with most rinse pH between pH 3.50 to pH 3.75, or above pH 7.0. Sampling from the interior of the dump showed that Fe concentrations are generally low, with the majority of the acidity associated with Al. Aluminum concentrations in dump pore waters were found to be in equilibrium with alunite [$KAl_3(SO_4)_2(OH)_6$], the presence of which was confirmed by XRD. Drainage emanating from the base of the dump shows higher pH in comparison to the dump interior, with Al concentrations being in equilibrium with gibbsite [$Al(OH)_3$]. Groundwater quality at the base of the dump interior alternates from alkaline during base flow conditions, to mildly acidic pH range during the spring freshet. The presence of alkaline water in the basal drain directly below an acidic waste rock dump is interpreted to reflect the seepage of alkaline groundwater into the basal drain during freshet conditions. Conversely, drainage emanating from the dump toe is concluded to result from the mixing of alkaline groundwater with acidic dump seepage in the basal drain.

Key Words: acidic drainage, neutral drainage, prediction, chemical evolution, mineral solubility

Introduction

A case study is presented which provides medium-term monitoring results from a segregated, PAG waste rock dump. The objective of this work is to present the results of a multi-disciplinary approach designed to identify and describe the geochemical processes within a large-scale waste rock pile that control the variability and quality of water discharging from the dump toe.

While waste rock construction is ongoing, portions of the pile are more than 25 years old. Recent flow and water quality from the past seven years are presented along with a more recent characterization of the dump interior. These include three, continuous profiles of waste rock pH and ABA characteristics, mineralogy, waste rock pore water, basal drain groundwater, and toe seepage. A diverse database is used to model mineral solubility and geochemical processes. Aluminum buffering reactions, solute mixing, and pH constraints are identified.

An historic waste rock dump provides a unique opportunity to investigate and identify geochemical processes controlling the fate and transport of waste rock seepage. This study underscores the importance of understanding water balance, groundwater, and waste rock geochemistry in order to determine and predict water quality emanating from a large-scale waste rock pile.

Site Description

The study area consists of a low-sulfide porphyry deposit in the central Rocky Mountains of North America. The mine includes an open-pit with two principal waste rock storage facilities. The region surrounding the study area has a sub-alpine climate, typical of high altitude inland mountains of the

western North America. The average ambient air temperature at site is approximately 4°C. Winters are cold with temperatures ranging from -34°C to -1.1°C. The summer months of June to August are typically cool and dry, with temperature maxima ranging from 10°C to 29°C. The average yearly precipitation is approximately 584 mm, most of which occurs as snowfall in the winter, although shorter duration rain events and thunderstorms are common in the summer months. Hydrology in the region is strongly influenced by snowmelt, which accounts for >70% of annual runoff from the surrounding catchments.

Geology

The lithologies present can be categorized into three general rock types: Eocene-aged volcanics; Paleozoic, marine-based, metasedimentary rocks; and Cretaceous plutonic intrusives which host the main ore body. The volcanics consist of a series of basaltic to dacitic lava flows, tuffs and breccias, while the metasediments consist of thinly bedded argillites and shales. The intrusive complex comprises lithologies that range from biotite granodiorite to biotite quartz monzonite. Sulfide mineralization is limited to the intrusive and metasedimentary rock types.

Historic data provides an indication of waste rock characteristics. Minor and major elemental abundances were quantified using aqua regia digestion/ICPMS and X-ray fluorescence (XRF) analysis, respectively. The mineralogical composition of the metasedimentary and intrusive rock types was determined by quantitative X-ray diffraction (XRD). The acid generating potential and acid neutralizing potential of these rock types were characterized by acid base accounting (ABA) methods to quantify sulfur species (acid potential) and Sobek neutralization potential (NP). Median ABA results are presented in Table 1; median aqua regia results for trace elements are presented in Table 2; and median XRF results for major elements are presented in Table 3.

Table 1. Median acid base accounting results for the three rock types composing waste rock.

Rock type	Sobek NP	Total S	NP/T-AP
	kg/t	wt. %	Ratio
Metasediments	10.2	0.48	0.7
Intrusives	8.7	0.39	0.7
Volcanics	11.8	0.75	0.5

Table 2. Median results of aqua regia extraction for the three rock types composing waste rock.

Rock type	Cu	Mn	Mo	Se	Zn	Ni	Pb	As	Cd	Co	U
	ppm	ppm	ppm	ppm	ppm	ppm	ppm	ppm	ppm	ppm	ppm
Volcanics	18.4	424	20.7	0.5	54	8.1	18.2	4.9	0.11	8	1.3
Intrusives	38.7	162	364	1.6	41	1.8	68.4	87.5	0.01	3.7	5.4
Meta	34.05	380	1.45	2.1	164	27.6	2.4	1.8	0.95	5.2	1

Table 3. Median results of XRF whole rock analysis for the three rock types composing waste rock.

Rock type	Al_2O_3	C_aO	Fe_2O_3	K_2	MgO	MnO	Na_2O	SiO_2	P_2O_5	TiO_2
	%	%	%	%	%	%	%	%	%	%
Intrusives	15.00	1.81	2.66	3.98	0.67	0.04	2.97	73.05	0.10	0.30
Metasediments	12.15	4.87	6.42	2.91	3.36	0.07	1.01	65.55	0.59	0.60
Volcanics	17.14	4.16	4.43	1.19	2.53	0.06	2.98	57.85	0.14	0.64

Sulfide minerals identified by XRD include pyrite and trace quantities of pyrrhotite. The XRD results identified calcite in the metasedimentary and intrusive rock types. The major rock forming minerals identified by XRD include quartz, plagioclase feldspar, K-feldspar and mica. These three minerals form more than 90% of the intrusive waste rock samples analyzed. Although the material was previously screened as PAG, ABA results suggest the waste rock is not overly reactive with relatively low total sulfur. Median NPR values are 0.7 or lower for all three rock types.

Dump Construction

Two waste rock facilities exist in the study area. The PAG pile, which is the subject of this paper, contains PAG material exclusively, while the NAG pile contains both PAG and NAG material. Drainage from the NAG pile and its comparison to PAG seepage water quality is the subject of a complementary paper published in this proceeding (Dockrey and Stockwell, 2012).

The PAG waste rock dump is a valley-fill, end-dump facility containing run-of-mine material from an adjacent open pit (Figure 1). Waste dump construction commenced in 1981 and is on-going. PAG segregation began in 1996. The base of the dump was constructed as a French Drain. Water quality and flow are measured at the toe of the dump. From the toe, the footprint of the dump occupies approximately 25% of the total catchment area. The dump contains approximately 118 million tonnes of predominantly PAG waste rock as well as low grade ore. A cross section of the dump is provided in Figure 2 which illustrates the basal French Drain and borehole locations.

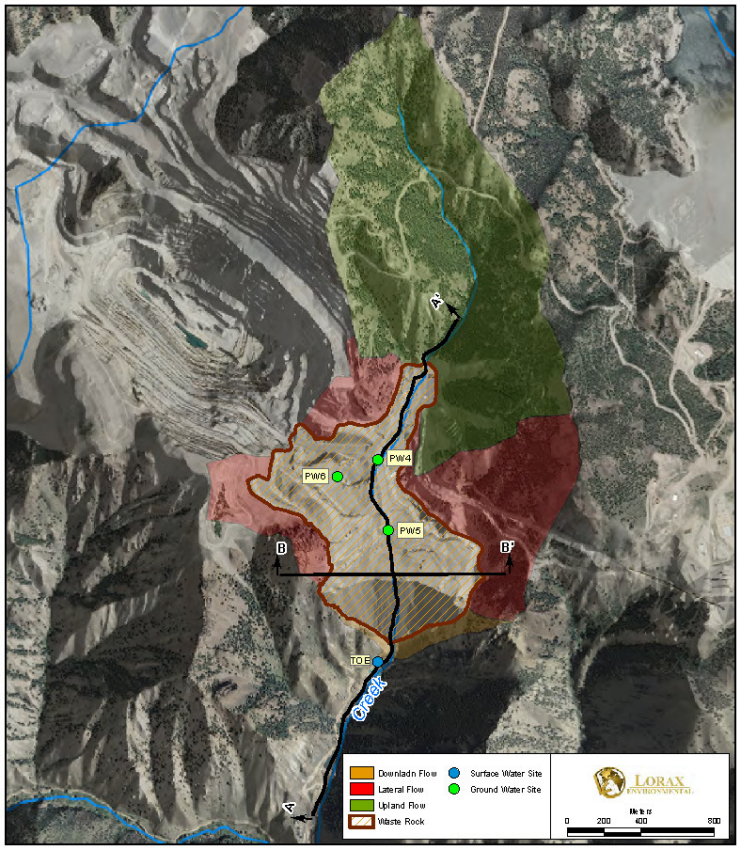

Figure 1. Location of PAG waste rock dump with borehole, monitoring, and cross-section locations. Drainage areas are also shown in yellow and red shading.

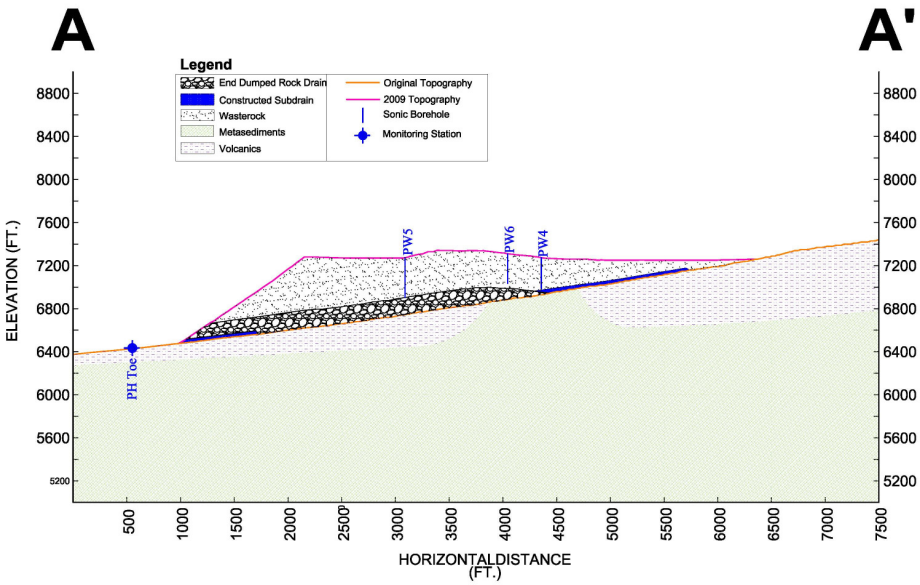

Figure 2. Cross-section A – A´ of the PAG waste dump with borehole and monitoring locations. The basal French Drain is also illustrated.

Methods

Waste Rock Characterization

Continuous logs of waste rock were collected at three locations within the dump interior using a 4-inch Sonic drill stem (Figure 1). Composite samples were analyzed for ABA paste pH, and selective leachate extractions (not shown). Following drilling, a groundwater well was installed at location PW4 and was screened within native overburden beneath the dump basal drain. Waste rock samples and a white precipitate forming in the toe drainage system were collected and submitted for mineralogical examination (Jambor, 2005).

Flow and Groundwater

Flow emanating from the waste rock facility has been measured continuously from a Parshall Flume since 2005. Manual water levels are also collected on a weekly basis, while continuous groundwater elevation data have been collected from well PW4 since 2005. Manual confirmatory water levels are measured quarterly.

Water Quality

Since September 2000, water quality monitoring of waste dump seepage at the toe of the dump (PHToe) has occurred on a weekly basis for a suite of parameters including pH, conductivity, dissolved oxygen, sulfate, Cd, Cu, Mn, and Zn (metals as dissolved). A full chemical analysis of dump seepage is performed less frequently (quarterly to monthly) and includes measurements of total and dissolved metals. Groundwater samples from well PW4 have been collected on an annual to quarterly basis for a full suite of chemical analysis.

Waste Rock Pore Water

Waste rock samples were collected from trenches, sieved in the field (<1/4"), sealed in plastic bags, and frozen. Sampling was conducted in the winter and targeted reactive zones identified by steam vents (Figure 3). Pore waters were extracted from a number of samples at the University of British Columbia in accordance with Unsaturated Flow Apparatus (UFA) Method of Technical Procedures (UFA, 1997) using a bench-top centrifuge. Extracted pore waters were filtered with a 0.45 um syringe filter and analyzed for sulfate and metals.

Figure 3. Reactive hot spots showing preferential snow melt on dump surface.

Results and Discussion

Hydrology and Hydrogeology

Flow from the toe of the dump shows a seasonal signature resulting from snowmelt (Figure 4). Waste dump drainage is produced from: 1) groundwater that is derived from recharge zones within the catchment above the waste rock pile; 2) surface water runoff that enters along the margins of the pile surface; and 3) precipitation (rain and snow) that falls directly on the dump surface and percolates through the waste pile. Groundwater elevations measured within the dump interior (PW4) illustrate the porous nature of the dump and the seasonal drain down that occurs following peak snowmelt each spring.

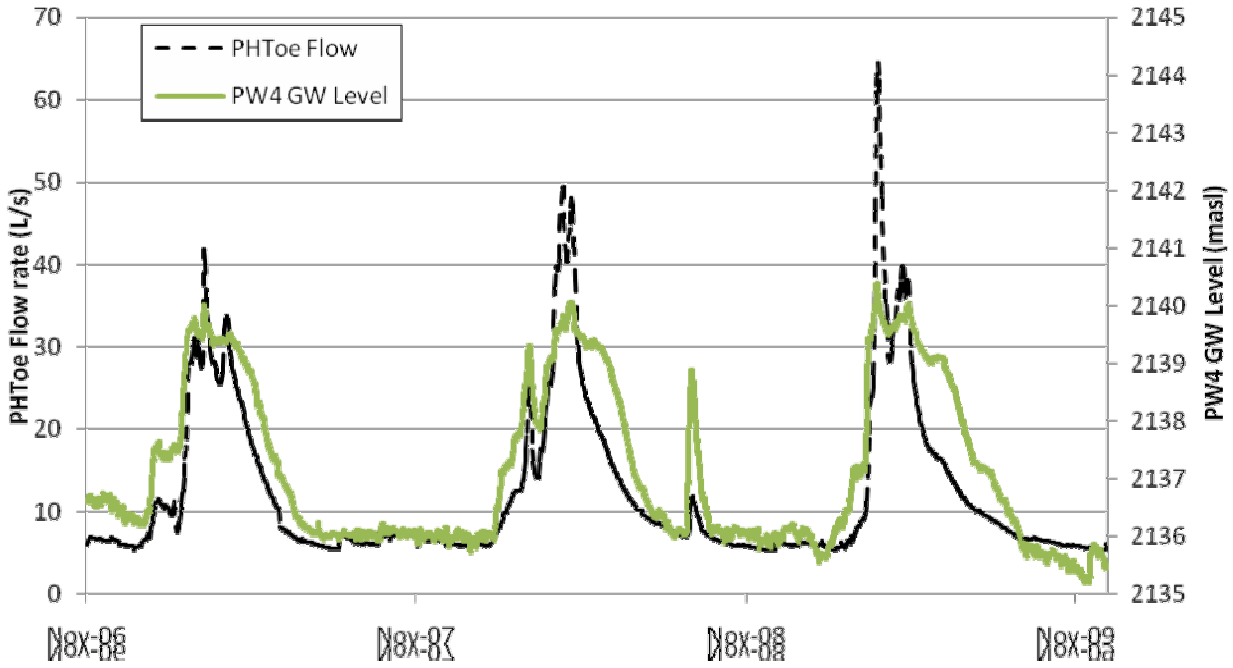

Figure 4. Plot illustrating seasonal signature of discharge and groundwater elevation from the waste rock toe (PHToe) and within the waste rock dump (PW4).

Dump Drainage Chemistry

Water quality and flow measured at the dump toe is depicted in Figure 5. Prior to 2003, water quality emanating from the dump was of reasonably good quality and circum-neutral pH. These conditions persisted until the spring freshet of 2003, when water chemistry changed abruptly and coincidently with peak spring discharge. A sharp decrease in pH followed along with an increase in dissolved metal and sulfate concentrations (Figure 5).

Following a period of transition, the pH of toe discharge stabilized and has remained at approximately pH 4.5 since 2006. Seasonal peak sulfate and metal concentrations coincide with snowmelt. Infiltration through the dump is rapid (Figure 4). Delayed drain down through the dump results in elevated concentrations that persist through the active flow season. Concentrations of sulfate and metals typically decrease with the onset of winter baseflow, which is influenced by the discharge of regional groundwater, as represented by PW4 (Figure 5).

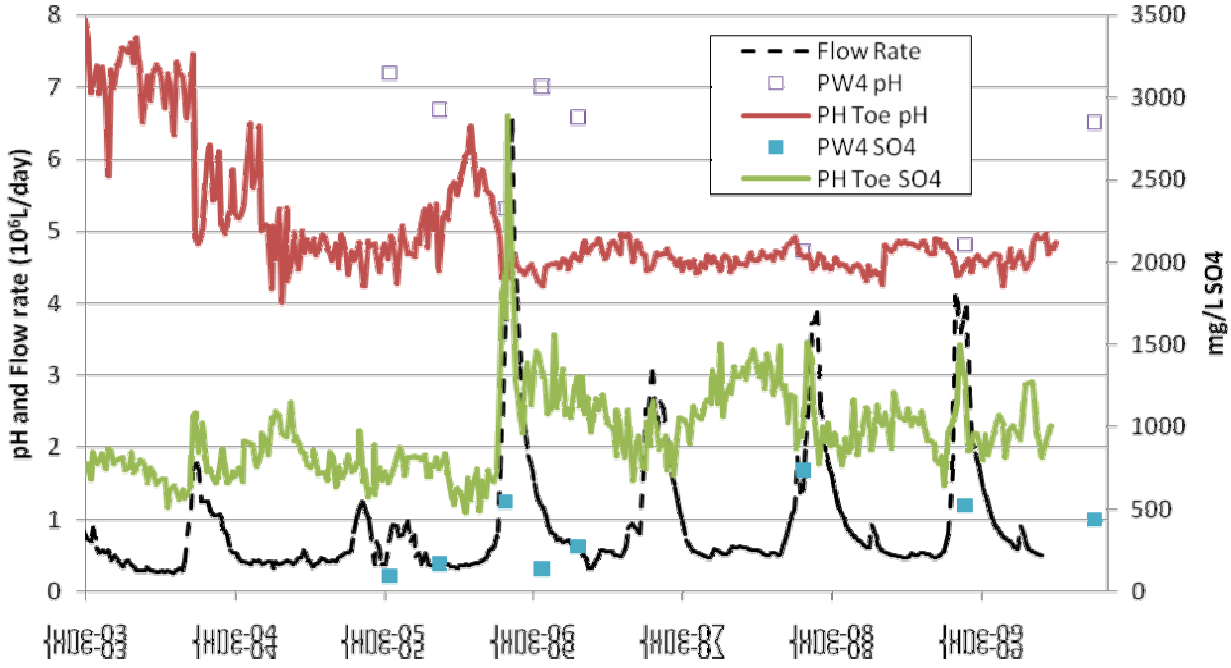

Figure 5. Time series of flow and water quality of dump discharge (PHToe) and internal dump groundwater (PW4)

Waste Rock Borehole Samples

Profiles of rinse pH and net NP (NNP) through the dump interior are presented in Figure 6. Boreholes PW4 and PW6 represent the oldest portions of the dump and contain waste rock material that precedes PAG separation. As well, the upper portion of PW6 includes the low-grade stockpile. These portions of the dump are less reactive as NP has been depleted and sulfides are largely exhausted (e.g., NNP=0). Borehole PW5 represents more recently deposited material, is the most acidic, and has largest amount of remaining acid generating potential (NNP < 0). At all locations, the internal pH of the dump does drop below pH 3.0 and suggests the dump seepage is buffered by aluminosilicate weathering, as discussed in subsequent sections. The upper portion of the waste rock pile is composed of non-acid generating rock, which was deposited as a hydrologically encapsulating non-acid generating layer.

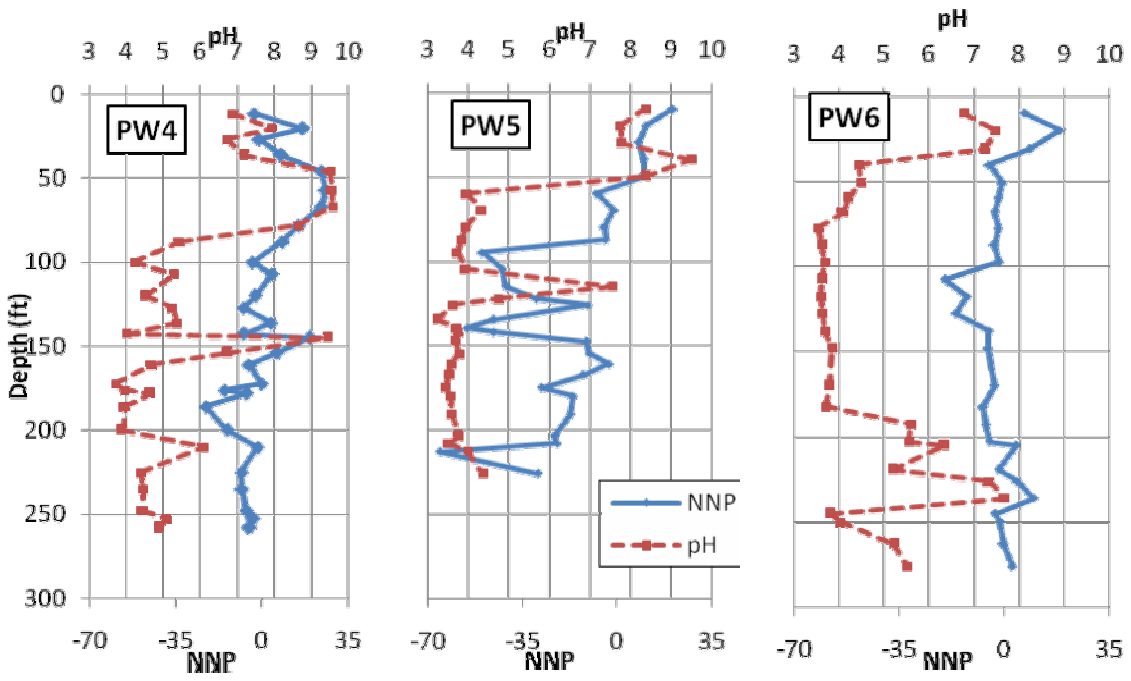

Figure 6. Rinse pH and Net-NP (NNP) profiles from waste rock boreholes PW4, PW5 and PW6.

Regions of the dump contain isolated portions of NP at depth that are surrounded by acid-generating materials (Figure 6). These areas are likely caused by capillary breaks within the dump interior which develop from the segregation of material during end dumping (Fala, *et al.* 2005). Geochemical heterogeneity is common in large-scale, coarse waste rock piles.

Dump Pore Water

Pore water data was collected from reactive zones within the waste rock dump and are summarized in Table 4. Water quality from toe seepage and groundwater (PW4) are provided for comparison. Dump pore water pH ranges from 4.2 to 2.6 and is more acidic and more elevated in metals than toe discharge and basal groundwater. In this regard, the pore water results provide a proxy for seepage quality percolating through the dump interior.

Table 4. Pore water geochemistry of waste rock samples (mg/L).

Sample ID	pH	Sulfate	Aluminum	Iron	Zinc	Manganese
1	2.6	9000	1270	2890	13.7	99.9
2	3.0	2520	265	63.5	8.8	82.3
3	3.2	1840	111	2.84	4.4	36.3
4	3.2	2130	109	2.95	4.3	35.6
5	3.3	1980	143	3.36	4.2	34.1
6	3.3	1790	102	2.51	2.1	19.1
7	4.2	2010	5.7	<0.06	1.4	19.5
PHToe	4.2 - 5.0	646 - 1806	6.6 - 60	<0.03 - 0.12	1.1 - 5.2	7.2 - 26.9
PW4	4.7 - 6.6	133 - 730	0.01 - 6.5	<0.03 - 0.04	0.02 - 1.4	0.11 - 15.5

Notes: Pore water samples were collected in 2006. PW4 and PH Toe concentrations are ranges observed from 2005 through 2010.

Mineralogy of waste rock associated with pore water and PHToe drainage quality are presented in Table 5. Jambor (2005) used X-ray diffraction and SEM-EDS to identify mineral precipitates commonly associated with ARD (Nordstrom, 1982). K-jarosite, for example, only forms in relatively acidic waters (pH <3.5). Conversely, goethite forms in more neutral waters, but is not readily dissolved when the pH becomes acidic. Alunite is a relatively insoluble Al-oxyhydroxide-sulfate mineral which precipitates under relatively acidic (pH 3 to 4) conditions. The white precipitate found within the toe drain was examined using SEM-EDS due to poorly resolved XRD pattern produced by the sample (Jambor, 2005). The EDS spectrum contained strong peaks for Al, O, and S and suggests an Al-SO_4 mineral.

Table 5. Mineralogical results of waste rock samples and white precipitate collected from PHToe.

Mineral	Formula	Waste Rock	PHToe
K-Jarosite	$KFe_3(SO_4)_2(OH)_6$	✓	
Alunite	$KAl_3(SO_4)_2(OH)_6$	✓	
Goethite	$FeO(OH)$	✓	
Gypsum	$CaSO_4 \bullet 2H_2O$	✓	
NA	Al-O-S*		✓

*Precipitate identified by SEM-EDS.

Iron and Aluminum Solubility Controls

Aluminum and Fe precipitates are typically the predominant pH buffering minerals in ARD environments as Al and Fe are both major carriers of acidity. Mineral solubility modelling was conducted in order to gain further insight on the nature of geochemical processes within and beneath the dump. Water quality was modelled using PHREEQC and the thermodynamic database Minteq.v4 (Parkhurst and Appello, 1999). Thermodynamic data for schwertmannite was added to the database from primary literature sources (Kawano and Tomita, 2001; Majzlan *et al.,* 2004). Solubility curves were developed for mineral precipitates of interest and compared to water quality observations. To account for activity and speciation reactions, a regression was developed which relates the dominant cation and anion (Ca and SO_4) to pH in drainage waters.

The interpretation of saturation indices (SI) for ferric iron oxides (e.g., ferrihydrite, schwertmannite, K-jarosite, and goethite) is complicated due to the lack of aqueous Fe data at varying oxidation states. At pH less than 3.5 the reduced oxidation state of iron (Fe^{2+}) becomes significant in sulfide oxidizing environments due to kinetic inhibition of Fe^{2+} oxidation by O_2 (Evangelou and Zhang, 1995). The ratio of Fe^{3+} to Fe^{2+} in ARD systems is mediated by microbial activity and is rarely in equilibrium (Baker and Banfield, 2003). The PHREEQC speciation model sets the ratio of Fe^{3+} to Fe^{2+} to be in equilibrium with atmospheric oxygen. This produces an overestimate of the Fe^{3+} to Fe^{2+} ratio, resulting in an overestimate of the SI of ferric iron oxides.

Measured concentrations of Fe are plotted against solubility curves of common iron precipitates in Figure 7. Iron concentrations in mine waste water are expected to be controlled by the solubility of iron oxides due to the abundance of iron in sulfide minerals and gangue rock which is associated with weathering of sulfide minerals. Secondary Fe minerals commonly associated with ARD waters include K-jarosite ($KFe_3(OH)_3(SO_4)_2$), schwertmannite ($Fe_8O_8(OH)_6SO4$), ferrihydrite ($Fe(OH)_3$), and goethite ($FeOOH$). Of these minerals, schwertmannite and ferrihydrite are relatively amorphous, while K-jarosite and goethite are more crystalline. In ARD environments, ferrihydrite and schwertmannite are the first minerals to form as a result of iron sulfide oxidation. As schwertmannite and ferrihydrite ripen or age, they transform to K-jarosite under relatively acidic conditions (pH<3.5) and to goethite at higher pH (pH>3.5) (Bigham *et al*., 1996).

Pore water samples at a pH >3.0 plot nearest the schwertmannite solubility line, while pore water samples at pH <3.0 plot near the ferrihydrite solubility line. Ferrihydrite is not expected to control Fe concentrations in acidic (*e.g.,* pH ≤ 3.0), sulfate-rich water (Bigham *et al.,* 1996). This is attributed to kinetic inhibition of Fe^{2+} oxidation under acidic conditions, leading to Fe^{2+} enrichment. Goethite and K-jarosite were found in pore water samples at a pH of 3.2 and 2.6; however, neither mineral is capable of reducing Fe concentrations to the point of equilibrium. Schwertmannite appears to be controlling the Fe concentrations in pore waters with pH >3.0 and toe discharge. The ageing products of schwertmannite transformation, K-jarosite and goethite, are forming within the pile but are unable to control Fe concentrations due to limitations in formation kinetics. From these observations, it is evident that iron-bearing precipitates are not the principle minerals responsible for buffering pH at PHToe.

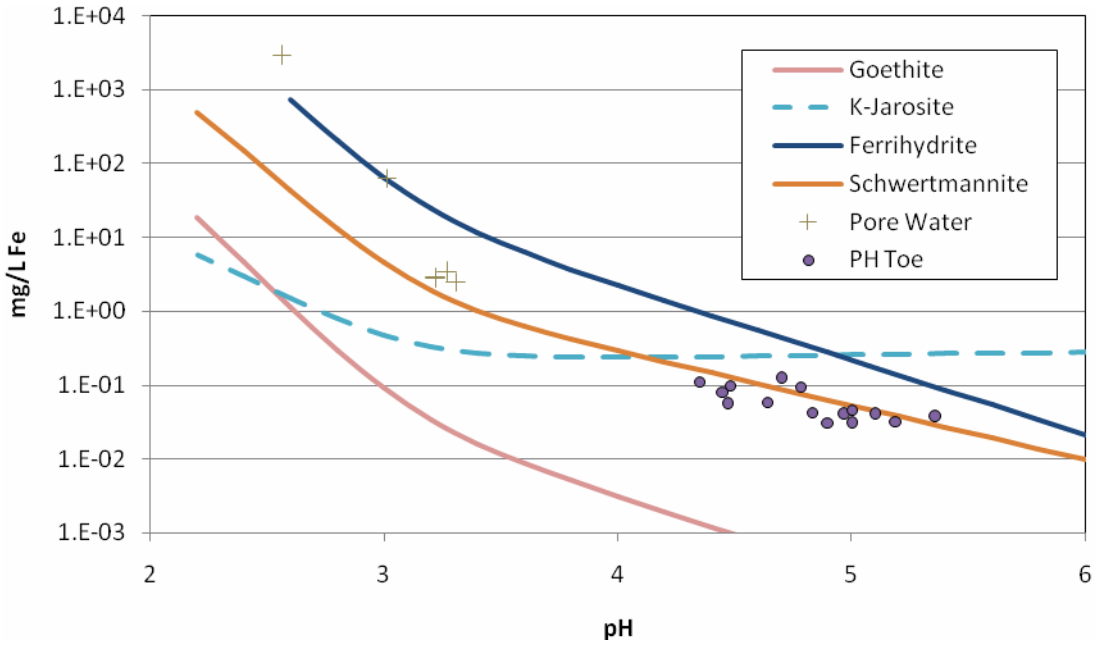

Figure 7. PHREEQC modelled iron solubility curves plotted with measured water quality from dump pore water and toe drainage (PHToe).

Dump toe drainage pH has remained between 4.5 and 5.0 since 2006 and is indicative of an aluminum buffered system. The Al minerals commonly associated with sulfate-rich waters include alunite ($KAl_3(SO_4)_2(OH)_6$), basaluminite ($Al_4(OH)_{10}SO_4$), hydrobasaluminite ($Al_4(OH)_{10}SO_4 \bullet 12\text{-}36H_2O$), amorphous Al-hydroxide ($Al(OH)_3$(am), and gibbsite ($Al(OH)_3$) (Nordstrom, 1982). Of these minerals, alunite and gibbsite are crystalline, while (hydro)basaluminite and $Al(OH)_3$(am) are relatively amorphous. Hydrobasaluminite dehydrates to basaluminite under room temperature conditions, and is considered a precursor to basaluminite formation. The formation of hydrobasaluminite and basaluminite is kinetically favored over other aluminum sulfate minerals, however (hydro)basaluminite is metastable, and known to transform to alunite over time (Nordstrom, 1982; Prietzel and Hirsch, 1998). Similarly $Al(OH)_3$(am) is metastable with respect to its polymorph gibbsite.

Aluminum mineral solubility curves are plotted against pH and compared to measured water quality in Figure 8. Pore water data aligns well with the alunite solubility curve and supports the notion that alunite is controlling aluminum concentrations. Note, however, that alunite is supersatured in PHToe waters, suggesting that alunite does not control Al concentrations in the basal drain (PHToe).

Most toe seepage and basal groundwater (PW4) data fall within the predicted range of gibbsite equilibrium. Groundwater (PW4) is acidic during high flow, and circum-neutral during baseflow. Acidic PW4 samples plot along the gibbsite solubility curve, while circum-neutral samples plot above the gibbsite solubility curve. As water flows from PW4 to PHToe along the underdrain of the pile, it accumulates significant quantities of Al (e.g., alunite equilibrium porewater) while remaining near equilibrium with gibbsite. Samples that plot above the solubility line are oversaturated with gibbsite, suggesting that gibbsite is precipitating in the PHToe drainage. All five neutral pH PW4 samples plot above the upper gibbsite solubility line, indicating that gibbsite is precipitating within the base of the dump during baseflow conditions (Figure 5).

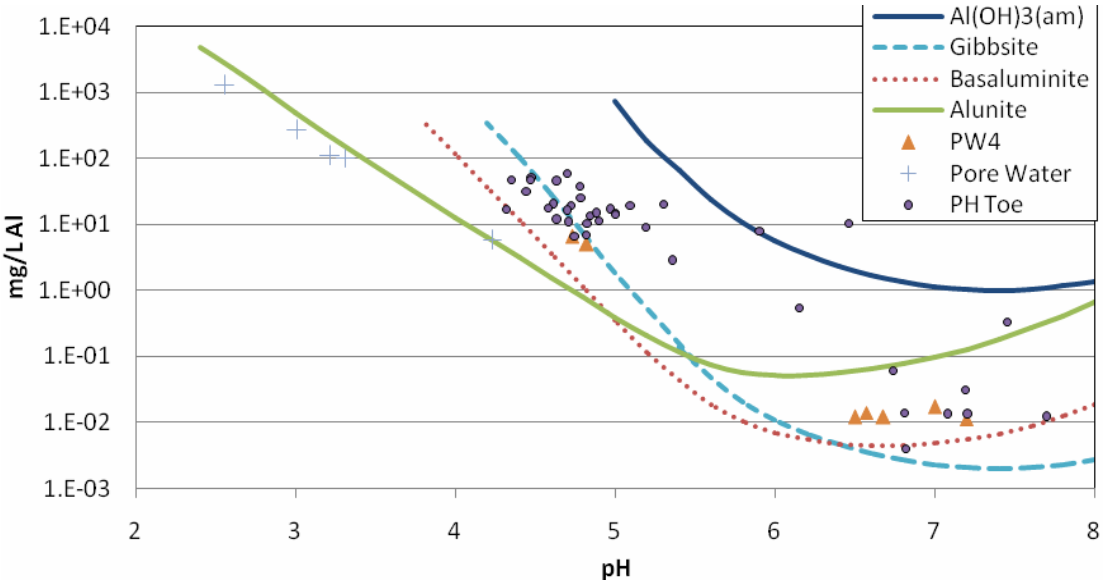

Figure 8. PHREEQC modelled aluminum solubility curves plotted with measured water quality from dump pore water and toe drainage (PHToe).

Based on multiple lines of evidence, the following conceptual model can be constructed. Pore water within the dump interior is in equilibrium with alunite, as supported by internal profiles of dump pH (Figure 6), waste rock mineralogy (Table 5) and solubility modeling (Figure 8). Pore water then discharges to the basal drain where it mixes with groundwater in the basal drain of the dump. During baseflow periods, the upper portion of the basal drain is circum-neutral (Figure 5) and results in the precipitation of gibbsite and subsequent buffering of Al and pH (Figure 8). Conversely, during peak flow conditions, the upper basal drain is mildly acidic. During this period in the hydrograph, alunite and basaluminite precipitate in the underdrain while gibbsite dissolves. As a result, pH, sulfate and aluminum concentrations remain relatively stable, despite the wide variations in seasonal flow rates.

It is apparent that gibbsite has been controlling Al concentrations and pH at PHToe since persistent ARD conditions developed in the spring of 2006. Gibbsite remains the dominant buffering mineral despite the presence of basaluminite. Basaluminite formation is not able to draw gibbsite out of equilibrium as long as solid phase gibbsite exists. These buffering reactions persist due replenishment of gibbsite during baseflow conditions when alkaline groundwater is discharging into basal drain.

Summary

Multiple lines of evidence were used to identify and constrain geochemical processes controlling the variability and quality of seepage emanating from a large-scale waste rock pile. Long-term monitoring

data combined with a detailed investigation of internal dump geochemistry provided a diverse database upon which to model mineral solubility and geochemical processes.

Results demonstrate that two distinct, seasonal phases occur. During baseflow conditions, Al-laden seepage mixes with alkaline groundwater in the basal drain and results in the formation of gibbsite, which buffers Al and pH in waters discharging from the dump toe. During peak runoff, snowmelt readily infiltrates into and passes through the waste rock dump. Groundwater in the basal drain is overwhelmed with this acidic pore water and results in the dissolution of gibbsite, and subsequent precipitation of basaluminite. Aluminum, pH and sulfate concentrations are buffered by these mineral reactions and remain relatively constant. These buffering processes are expected to persist as long as alkaline groundwater continues to discharge to the underdrain and replenish the reservoir of gibbsite during baseflow conditions.

These results underscore the importance of taking a multi-disciplinary approach in the characterization of large-scale waste rock piles and the prediction of their effects on water quality.

References

Baker, B. J. and Banfield, J. F. (2003), Microbial communities in acid mine drainage. FEMS Microbiology Ecology, 44: 139–152.

Bigham, J.M., Schwertmann U., Triana, S.J., Winland, R.L., Wolf, M. 1996. Shwertmannite and the chemical modeling of iron in acid sulfate waters. Geochimica et Cosmochimica Acta, 60, pp. 2111-2121.

Blowes, D.W., Ptacek, C.J., Jurjovec, J., (2003). Mill tailings: hydrogeology and geochemistry. In: Jambor, J.L., Blowes, D.W., Ritchie, A.I.M. (Eds.), Environmental Aspects of Mine Wastes, Short Course Volume 31, Mineralogical Association of Canada, pp. 95-116 (chapter 5).

Evangelou, V.P., Zhang, Y.L., (1995). A review: pyrite oxidation mechanisms and acid mine drainage prevention. Critical reviews in Environmental Science and Technology, 25, 141-199.

Fala, O., Molson, J., Aubertin, M., Bussiere, B., 2005. Numerical modelling of flow and capillary barrier effects in unsaturated waste rock piles. Mine Water and Environment, 24, 172-185.

Jambor, J.L. (2005) Mineralogical investigation of waste rock samples from a porphyry deposit. Prepared by Dr. John L. Jambor for Lorax Environmental Services Ltd., March, 2005. 10 pp.

Kawano, M., Tomita, K., (2001). Geochemical modeling of bacterially induced mineralization of schwertmannite and jarosite in sulfuric acid spring water. American Mineralogist, 86, 1156-1165.

Morin, K.A., Hutt, N.M., (2000). Discrete-zone mixing of net-acid-neutralizing and net-acid-generating rock: Avoiding the argument over appropriate ratios. In: Proceedings from the Fifth International Conference on Acid Rock Drainage, May 20-26, Denver, USA, Volume II, p. 797-803. Society for Mining, Metallurgy, and Exploration, Inc., Littleton, CO, USA. Page 797

Nordstrom, D.K., (1982). The effect of sulfate on aluminium concentrations in natural waters: some stability relations in the system Al2O3-SO3-H2O at 298°K. Geochimica et Cosmochimica Acta, 46, 681-692.

Parkhurst, D.L., Appelo, C., (1999). User's guide to PHREEQC (version 2)-a computer program for speciation, batch-reaction, one-dimensional transport, and inverse geochemical calculation. USGS, Water-Resour. Invest. Rep. 99-4259.

Stockwell, J.S., Dockrey, J.W., (2011). Aluminum buffering and geochemical equilibrium of seepage from a mildly acidic waste rock dump – long-term observations and implications for future water quality. In, Proceedings of the 9th International Conference on Acid Rock Drainage, May 20-26, 2012, Ottawa, ON, Canada.

UFA (1997). The unsaturated flow apparatus method for extracting pore fluids from relatively impermeable and highly unsaturated porous media. Unsaturated Flow Apparatus Ventures Inc. (UFA), Richland, Washington, pp 1-7.

Acronyms

EDS = energy-dispersive X-ray spectroscopy
XRF = X-ray fluorescence
XRD = X-ray diffraction